Korean J. Chem. Eng., 34(12), 3142-3149 (2017)
DOI: 10.1007/s11814-017-0174-2

pISSN: 0256-1115
eISSN: 1975-7220

Efficiency evaluation of the photocatalytic degradation of zinc oxide nanoparticles immobilized on modified zeolites in the removal of styrene vapor from air

Hossein Ali Rangkooy*,, Mojtaba Nakhaei Pour**,†, and Behzad Fouladi Dehaghi****

*Environmental Technologies Research Center, Ahvaz Jundishapur University of Medical Sciences, Ahvaz, Iran
**Department of Occupational Health, Health Faculty, Ahvaz Jundishapur University of Medical Sciences, Ahvaz, Iran
(*Received 4 April 2017 • accepted 24 June 2017*)

Abstract−Styrene monomer is a volatile organic compound that has many applications in plastics, rubber, and paint manufacturing industries. Exposure to styrene vapor has certain effects, including suppression of the central nervous system, loss of concentration, weakness and fatigue, and nausea and there is a possibility of carcinogenesis in long-term exposure. Therefore, it is necessary to control and eliminate this vapor. The aim of this study was to investigate the performance of zinc oxide nanoparticles on modified natural zeolites in removing styrene vapor from the air. Natural zeolites of clinoptilolite were modified using hydrochloric acid and diphenyldichlorosilane. Next, zinc oxide nanoparticles with different ratios of 3, 5, and 10 wt% were stabilized on the zeolites. To determine their characteristics, samples were used from BET, SEM and XRD analyses. The input styrene concentration and the ratio of nanoparticles stabilized on zeolites were studied as effective functional parameters on the removal process. The efficiency results of natural zeolites (Ze) and modified zeolites (Mze) in styrene adsorption from the air show that the styrene breakthrough in the bed of MZe compared to that of Ze increases approximately two times. Also, the results showed that the removal by the process of UV/MZe-ZnO 3%, UV/MZe-ZnO 5%, and UV/MZe-ZnO 10%, was 36.5%, 40%, and 26%, respectively. From the results it can be concluded that MZe can increase the efficiency of photocatalytic degradation. Clinoptilolites of Iran can be used as an adsorbent to remove polluted air in industries that have low concentrations and flow rates.

Keywords: Photocatalytic Degradation, Zinc Oxide Nanoparticles, Styrene, Zeolite

INTRODUCTION

Owing to industrial development and production of various materials (especially petroleum derivatives), occupational exposure to volatile organic compounds (VOCs) has increased. For VOC emissions, control can be used other than the methods of degradation and recovery such as adsorption, catalytic or thermal oxidation, absorption, and photocatalytic oxidation [1,2]. As an advanced oxidation process, photocatalysts provide a promising new technology for the decomposition of VOCs in air and water [3]. The photocatalytic process includes activation semiconductors by UV or appropriate visible light radiation and the formation of hydroxyl radicals oxidizing. The efficiency of photocatalysis depends on the process of separating electrons from the semiconductor and the process recombination of the pair hole-electron [4]. In the past few decades, heterogeneous photocatalysts have been used for the degradation of organic pollutants as a successful method and an appropriate alternative degradation process [4-6]. In heterogeneous photocatalysis, a known method for advanced oxidation processes, by excitation of a semiconductor (e.g. ZnO or TiO_2) with UV light or photons, the electron-hole pair will produce hydroxyl radicals to eliminate various pollutants in a randomized process [7-9]. Titanium dioxide (TiO_2) has been the most widely studied material in the field of photocatalysis [10,11]. However, ZnO shows photocatalytic activity similar or sometimes even better than that of TiO_2 and it is considered as a very promising alternative. Owing to the high the luminous sensitivity, non-toxic nature, high stability, polar property, a large band gap energy (3.37 eV), and high ability to produce electrons, this semiconductor has attracted special attention. The amount of the photolitic energy of radiation that is dependent on their power density of radiant energy is more important in photocatalytic excitation [12-14]. Despite the advantages of semiconductors, their use is limited due to their low surface area, low adsorption capacity, and operational costs [15]. Stabilization of semiconductors with a proper foundation due to increasing charge separation, increasing lifetime of charge carriers, increasing transfer of load surface in terms of the adsorbent substrates, and reducing cost can be overcome by these limitations [8,16]. Various types of supports may be used: activated carbon [17], activated alumina [18], and zeolites [19]. Zeolites, due to the three-dimensional structure, crystalline, high physical and chemical resistance, uniform cavities and channels, a high level and excellent adsorption ability and the unique structure are perfect support for this work [20]. Using methods such as chemical and thermal modifications can be controlled through the physical and the chemical characteristics of natural zeolites and increased their adsorbing efficiency [21-23]. The results of studies show which stabilization of photocatalysts on the adsorbent enhances the pollutant removal efficiency [24-26]. Ichiura's study to increase the efficiency of the photocatalyst system is proposed, where system performance will be much better if a primary

†To whom correspondence should be addressed.
E-mail: nakhaeimojtaba13@gmail.com

adsorbent, such as zeolites or activated carbon, is used as a photocatalyst bed [27]. The use of catalysts, especially catalysts such as titanium dioxide and zinc oxide, has been expanded to oxidizing properties of the sorbent and much research has been carried out in this regard. In addition, other methods can be used to increase the strength catalysts [28]. In this technique, using different radiation, especially ultraviolet radiation by producing electron-hole pairs on the zinc oxide, raises its oxidation strength, which is called the optical analysis system [29]. VOCs are the most common air pollutants, and their elimination poses challenges before researchers. Styrene monomer, a volatile organic compound, is considered one of the most important materials used in plastics and rubber industries [30]. According to a survey, workers of fibreglass and reinforced plastic industries are exposed to concentrations between 20-300 ppm [31]. Styrene health effects have been reported to vary widely among different organizations of health and safety. According to the Environmental Protection Agency, acute exposure to styrene monomer creates effects such as suppressing the central nervous system, loss of concentration, weakness, fatigue, and nausea [32]. This material probably belongs to the carcinogenic category [33]. Long-term exposure to styrene can also damage the reproductive system [34]. According to the standard of the American Conference of Governmental Industrial Hygienists (ACGIH), occupational exposure limit for eight-hour daily and 40-hour working week is 20 ppm, while the short-term occupational exposure limit is 40 ppm [35].

This study was conducted to investigate the performance of zinc oxide nanoparticles coated on zeolites for the removal of styrene vapor from polluted air. All experiments were conducted at room temperature (25±1 °C). Testing and implementation was set up at the laboratory of Ahvaz chemical agents.

MATERIALS AND METHODS

1. Materials

In this study, natural clinoptilolite granules of Semnan Garmsar mines (Iran) with a diameter of 0.5-1 mm were used. Styrene (purity>99.98%) and diphenyldichlorosilane were purchased commercially from Merck Germany. Zinc oxide nanoparticles with a size of 10 to 20 nm (made in America) were prepared from Pishgaman Nano-materials Company of Iranian. Other required materials, such as hydrochloric acid and toluene, were from Merck, Germany.

2. Characterization of Photocatalysts

Characterization of all samples was byd using scanning electron microscopy (SEM), X-ray powder diffraction (XRD) and surface area measurement (BET). The X-ray diffraction (XRD) pattern record used Model X PERT PRO MPD construction Panalytical Company. The wavelength of the device is 1.54 A with the producer 40 Kv, 40 mA which samples were scanned in 2θ of 4-80. Determination of the specific surface area and pore size was from the BET Quantachrome Chem device. The morphology of products and the confirmation of nanoparticles stabilization on zeolites involved using a field emission scanning electron microscope (FESEM) MIRA3TESCAN-XMU model, manufactured by America TSCAN, equipped with facilities of energy dispersive x-ray (EDX) with a voltage of 15 Kv.

3. Chemical Modification of Zeolites

Before being modified by chlorosilane, natural zeolite samples were washed by hydrochloric acid 2 M and prepared to the acid form (H). In this method, natural zeolites are transferred to the beaker containing 2 M HCl and then placed for an hour on a heater equipped with shakers at 75 °C. Then, it was filtered by Whatman

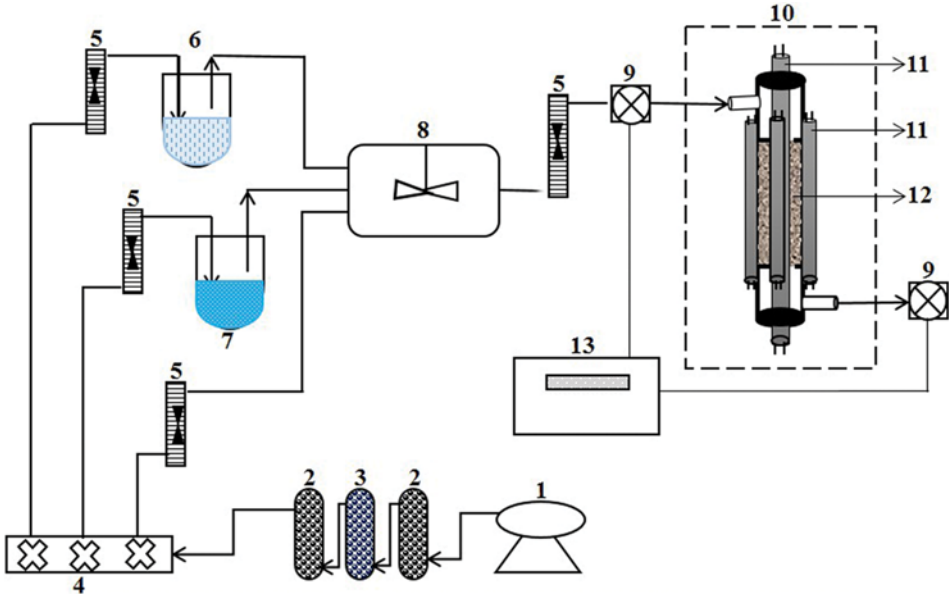

Fig. 1. Experimental schematic.

1. Air pump	4. Branch wall boxes	7. Water container	10. Photocatalytic reactor	13. Analyzer
2. Active carbon	5. Rotameter	8. Mixing tank	11. UV lamps	
3. SILICAGEL	6. Styrene container	9. Sampling port	12. Catalyst	

filter paper and washed with the necessary amount of hot distilled water and then cold distilled water to reach pH=7 and placed for drying at 100 °C in an oven for 24 hours. As many as 10 g of modified zeolites by HCL was weighed into a two or three-necked flask and 40 ml of toluene as a buffer. Next, 92 mmol of diphenyldichlorosilane was added to zeolites. The container of the mixture was placed under reflux conditions and passing of nitrogen on the liquid surface. The mixture was heated under nitrogen atmosphere in controlled temperature (10 °C below boiling point of the most volatile component) for 24 h. After completion of reaction time, the solid phase, which was modified zeolite, was separated by Whatman paper from the liquid phase and washed with distilled water and acetone. Then, the samples were placed at 105 °C oven for 24 hours and placed in the desiccator for maintenance and keeping cool [36,37].

4. Photocatalytic Removal System Design and Analysis

Fig. 1 shows the experimental system used in this study. The whole system hads three parts: 1) input section, removal or absorption section, and sampling section.

A dynamic system was used to provide air containing styrene in desired concentrations. In this method, the inlet air is passed by a 51w pump with a pressure of 11.147 mmHg (manufacturing Co. Hitachi Ltd.) from the container containing activated carbon and silica gel (to remove the inlet air pollution), and then, it is entered into the humidification system and the system of concentration. First, styrene vapor is cleaned and dried by the blowing air flow by a pump with a constant flow rate of 1 L/min in a container of the styrene solution during the evaporation emissions; then, it is entered into the mixing container and mixed with the air containing humidity and clean air, while a specified concentration is sent to the reactor containing the bed. A cylindrical reactor made of quartz glass (for full transfer of radiation of UV) with a length, diameter, and a thickness of 280 mm, 20 mm, and 2 mm, respectively, is used. This reactor has an inlet and outlet at a distance of 2 cm from both ends of the cylinder in such a way that they are in the opposite direction of each other. Hence, an 8-watt lamp is placed inside (center of the reactor) and three 6-watt UVA lamps are placed outside the reactor. The distance of the lamp inside the reactor to a surface inside the reactor was set to 3 mm and the distance of the outer lamps until the outer surface of the reactor body was set to 50 mm. The MZe-ZnO catalyst is placed within the reactors and around the inner lamp. Next, the air flow-containing styrene is passed through at a certain temperature, humidity, flow rate, and concentration. The concentration of styrene is measured and recorded in the inlet and outlet of the reactor at regular time intervals (5 min) by direct reading devices of phocheck Tiger (model 5000 made in England). The device works by the photo ionization detector (PID). To ensure the precision of the obtained data, any of the measurements are repeated at least three times. And to ensure the accuracy of the measured data in every few examples, these concentrations are once measured by gas chromatography (Philips PU4410) equipped with the FID detector.

5. Immobilization of ZnO Nanoparticles on the Modified Zeolite

Loading of ZnO nanoparticles on the modified zeolite adsorbent with weight ratios of 3%, 5%, and 10% was as the following: For preparation of 10 g of MZe/ZnO 5%, 0.5 g from zinc oxide was weighed and poured into the flask to create a uniform suspensions and thus was placed in ultrasonic devices for 30 min. Next, 9.5 g from modified zeolite was added to a suspension-containing nanoparticles and continuously put on a shaker for 22 to 24 hours until completely mixed and zinc oxide nanoparticles stabilized on the surface and pores of zeolite. Next, it was passed through a filter paper and dried at 80 °C, after which it was placed for calcination in the oven for 2 hours at 450 °C. MZe/ZnO 3% and MZe/ZnO 10% catalysts were prepared, each with known amount of ZnO and MZe content.

RESULTS AND DISCUSSION

1. Characterization of Samples

1-1. Measurement of a Surface

Table 1 shows The Brunauer-Emmett-Teller (BET) surface area of the MZe-ZnO catalysts decreased by increasing the amount of zinc oxide. Since, ZnO coating on the surface and Mze pores have blocked some of mesopores and micropores, thus slightly reducing the surface area and the average pore diameter of zeolite. In general, the surface catalyst is the most important affecting factor on the catalytic activity of the catalyst. The high surface area is only one of the factors contributing to the high efficiency of the adsorber to adsorb pollutants, but the destruction of organic pollutants in ZnO is a factor to compensate for the lower surface and subsequently a higher efficiency than the MZe catalyst [38]. Table 1 also shows that the modifying zeolite surface area had increased 2.47 times. The BET results show that the modification of zeolite by diphenyldichlorosilane improves and upgrades naturally the zeolite pore structure. This result is consistent with the study of Asilian et al.

1-2. Electron Microscope Scan Images of Photocatalyst Surface Morphology

Field-emission scanning electron microscopy (FESEM) is widely used to determine the morphology, shape, and approximate particles size in dimensions of nano and micro. Fig. 2 shows FESEM images of bed before and after the modification as well as after the immobilization process of nanoparticles on it. Fig. 3(c) shows the zeolite beads coated with zinc oxide nanoparticle. This implies the success of the immobilization of nanoparticles on zeolites. Also, a

Table 1. Properties of catalyst surface

Sample	Raw zeolite (Ze)	MZe	MZe/ZnO 3%	MZe/ZnO 5%	MZe/ZnO 10%
BET (m^2/g)	56.48	139.755	133.84	132.610	126.91
The average pore diameter (A°)	38.43	66.43	63.17	61.108	52.270
Total volume (cm^3/g)	0.1105	0.15129	0.14992	0.14701	0.13801

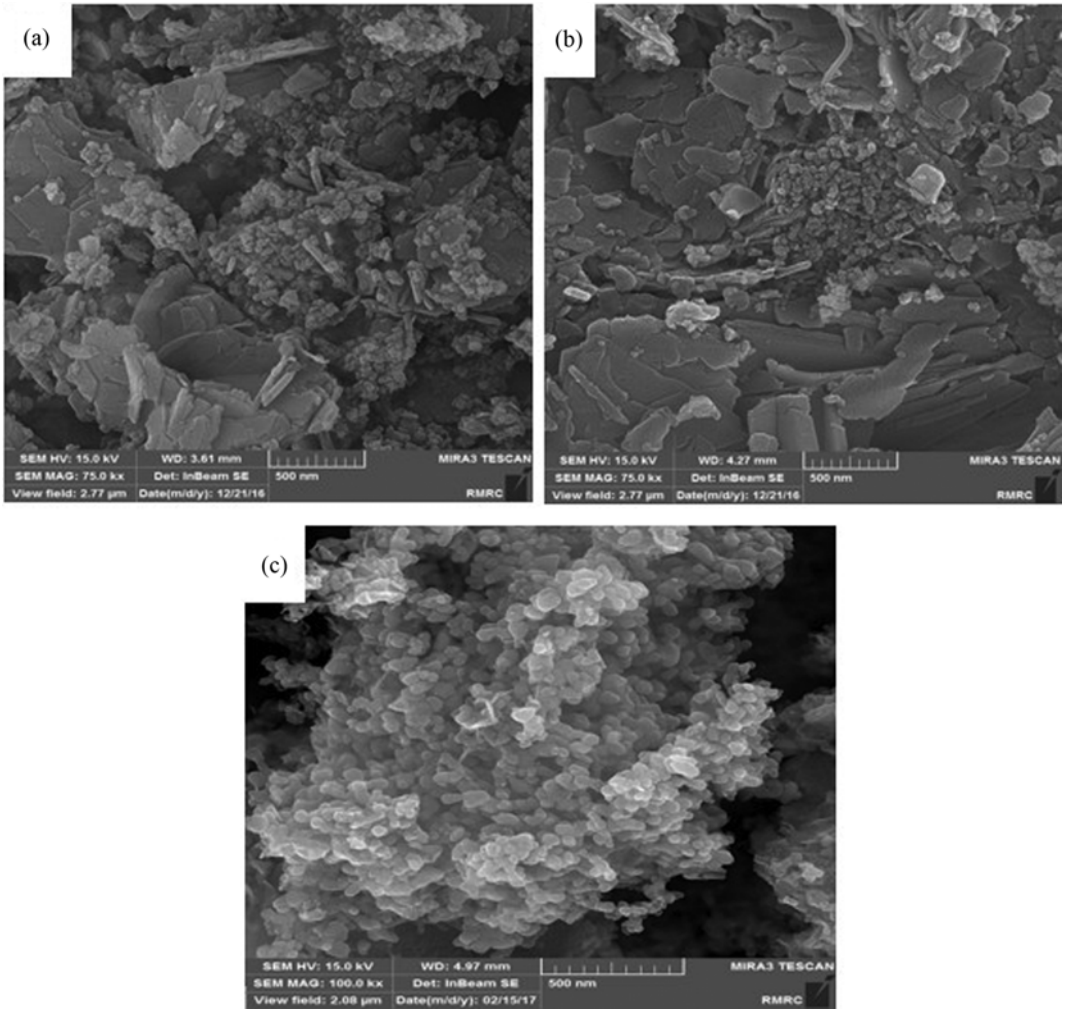

Fig. 2. FESEM image from (a) Ze; (b) MZe; (c) MZe-ZnO.

comparison of images of natural and modified zeolite shows that they are different in terms of outward appearance. It is clear, if the distribution of the nanoparticles on the catalyst surface is done more uniform, Photocatalytic reaction is better done. FESEM images are indicators of uniform-coating photocatalyst ZnO nanoparticles on zeolite.

Also in this study, elemental analysis of the samples was done using SEM-EDX. The results of this analysis are shown in Table 2. The results show that silica and aluminium are important elements that are present in the zeolite studied. Natural zeolites used in this study have 28.65% silica and 5.25% aluminium. But the modified zeolite has 30.34% silica and 3.59% aluminium. One of the effective factors on the adsorption of zeolite is ratio of Si/AL [39]. This ratio in natural zeolites is 8.45 and in modified zeolite 5.45, with the latter being increased three units compared to natural zeolites. Therefore, there is a significant increase in modified zeolite to reach the breakthrough and consequently increase the adsorption capacity until the breakthrough and saturation point. This ratio at MZe-ZNO 5% was shown to increase slightly. Fig. 3 shows the peak ingredients of MZe-ZNO 5% bed. The largest peak shows silica and smaller peaks show aluminium and zinc oxide.

Table 2. Elemental analysis of the samples

Element	Wt (%)		
	Ze	MZe	MZe-ZnO 5%
O	50.20	57.65	52.15
Na	2.11	0.63	1.96
Al	5.25	3.59	3.64
Si	28.65	30.34	31.58
Au	10.69	6.55	5.1
K	1.75	1.25	1.37
Fe	1.35	-	-
Zn	-	-	3.85

1-3. Crystal Structure of Photocatalysis

X-ray diffraction (XRD) is used to detect minerals in a sample usually. XRD, in addition to showing the crystalline structure of materials, can show any structural changes caused by physical and chemical effects te on materials. Fig. 4 shows the XRD patterns in different beds. The XRD pattern of natural samples shows that the main phase of the zeolites is from the clinoptilolite family. However,

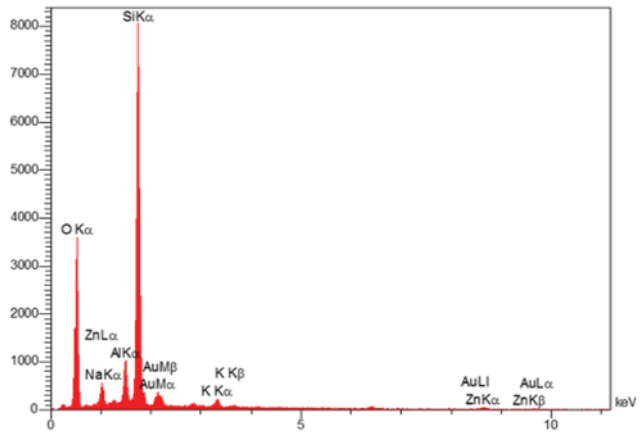

Fig. 3. EDX analysis of MZe-ZnO 5%.

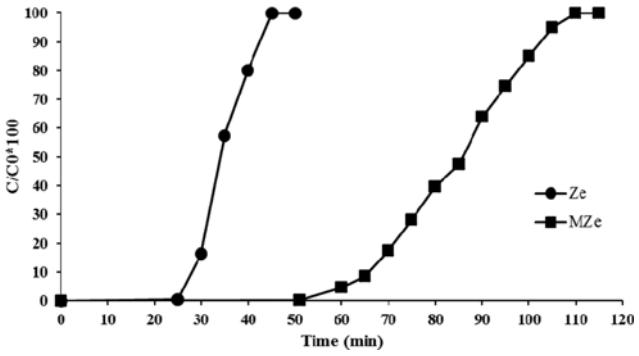

Fig. 5. Adsorption of styrene by natural zeolite (Ze) and modified zeolite (MZe). (C0=20 ppm).

short peaks seen from quartz and heulandite crystals hat in modified zeolite, the peaks of these phases are shorter or cannot be seen. Also, the crystal structure of ZnO nanoparticles in the XRD pattern is shown on a modified zeolite. The peaks of 2θ=34.4 and 2θ= 36.3 are related to crystal of ZnO.

2. The Effect of Modifying of Zeolite on Styrene Vapor Adsorption

In this study, the effectiveness of the modification of zeolite is shown by diphenyldichlorosilane. Zeolites are modified by a reaction between zeolite surface silanol groups and chlorosilane and, consequently, the stable covalent bond between the silane of organic and inorganic. Fig. 5 shows the efficiency results of natural and modified zeolites in styrene adsorption from the air are based on the emergence styrene in the reactor output. In a reactor containing natural zeolites, styrene emerged after 25 minutes and was saturated after 45 min. But in the reactor containing modified zeolite, styrene emerged after 51 minutes and was saturated after 105 min. The SEM images and BET measurements clearly represent the changes of physical and chemical properties of the modified compared to the natural Zeolite. Modifying of zeolite causes increased surface area, the average pore diameter and total volume of zeolite and this can cause increase of styrene adsorption. Huttenloch et al. investigated the adsorption of volatile organic compounds modified by clinoptilolite and diatomite with silane compounds. Their results indicate that if the phenyl group surface of modified clinoptilolite and diatomite with diphenyldichlorosilane was more inclined to combine with VOC than the other silanes, then the removal rate was higher [36,37].

3. Effect of the Loading of Zinc Oxide on Styrene Removal

MZe-ZnO photocatalysts were prepared with different loadings of ZnO until they were identified with photocatalyst with a higher efficiency. Fig. 6 shows the effect of ZnO loading on the styrene remove. The appearance point of styrene in the output of the reactor-containing process UV/MZe-ZnO 3%, UV/MZe-ZnO 5%, and UV/MZe-ZnO 10% was 59, 63, and 45 minutes, respectively. Also, the results show that the styrene removal by UV/MZe-ZnO 3%, UV/MZe-ZnO 5%, and UV/MZe-ZnO 10% catalysts was 36.5%, 40%, and 26%, respectively. The results indicate that increasing wt% of ZnO loaded on MZe from 3 to 5 wt%, leads to increasing styrene removal efficiency. These experiments demon-

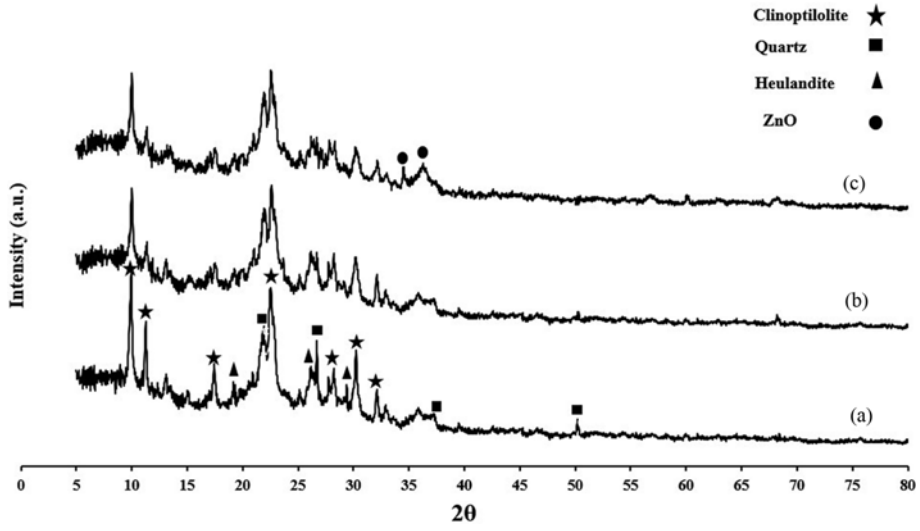

Fig. 4. XRD patterns of: (a) Zeolite, (b) modified Zeolite, (c) MZe-ZnO 5%.

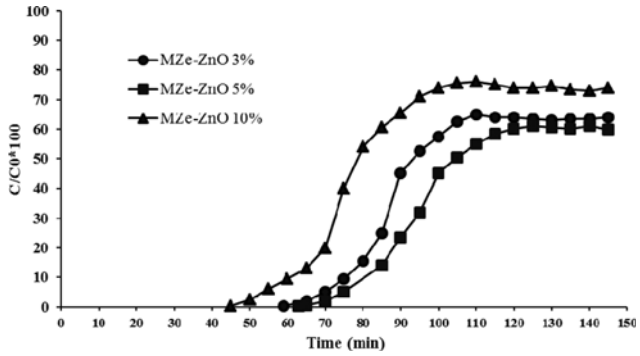

Fig. 6. Effect of nominal catalyst ZnO amount on rate photo-degradation of styrene (C0=20 ppm).

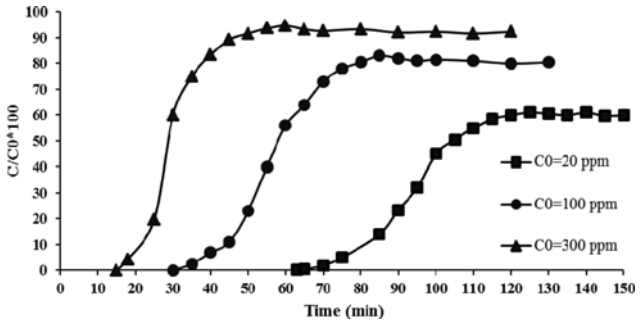

Fig. 7. Effect of concentration on photo-degradation reaction of styrene.

strated that the composites with very low amount of ZnO loading did not show sufficient photocatalytic activity, and also both modified zeolite and photocatalyst such as ZnO were needed for the effective destruction of styrene. This observation can be interpreted as that by increasing the catalyst amount causes to increase the number of active sites on the photocatalyst surface and subsequently increases the number of active radicals, and this increases the photocatalytic removal efficiency by increasing the generation of more active species for photocatalytic activity. Also, the results indicate that increasing wt% of ZnO loaded on MZe from 5 to 10 wt%, leads to decreasing styrene removal efficiency. This finding can be interpreted as that by increasing nanoparticles of zinc oxide on zeolite, the pores and cavity of zeolite (bands or agents of adsorption) are blocked and this causes reduced adsorption of styrene and less rate of styrene contact with ZnO and then reduced styrene removal efficiency. With zeolite, removal of styrene from air occurs only due to adsorption, because it does not have any photoactivity. On MZe-ZnO catalysts, both processes, adsorption of styrene by zeolite and its degradation by ZnO photocatalysts, occur at the same time. Since the adsorption process onto zeolite proceeds much faster than the degradation by the photocatalysis, the removal of styrene in the first occurs mainly by the former process. Gradual increase in removal of styrene is by both processes, i.e., adsorption and degradation. Therefore, the ZnO loading has a synergetic effect in styrene removal. Also, modified zeolite as a support can improve the photocatalytic activity of ZnO. In this study, the maximum activity of MZe-ZnO catalysts was achieved at 5 wt% of ZnO loading amount. In a similar study, Khatamian et al., the best rate of loading of ZnO on HZSM-5 in order to remove 4-nitrophenol in aqueous solution reported 7%. The more the percentage of ZnO (>7%) loading on HZSM-5, the less the rate of adsorption and elimination [40]. Researcher optimal amount of catalyst on supports was reported different [41,42].

4. Effect of Concentration on the Efficiency of Photocatalytic Removal

Inlet concentration has been one of the factors affecting the photocatalytic reaction, and it determines the mass transferred to the bed. In this experiment, the efficiency of the photocatalytic reactor contains 5 gm Mze-ZnO 5% photocatalyst was compared in three concentrations of 20, 100, and 300 ppm and in a constant flow of 1 L/min. As can be seen from Fig. 7, styrene vapor reduction in the concentration of 20 ppm in the first 65 minutes of testing was 97%, which decreased after about 115 minutes to 40%. In a concentration of 100 ppm, styrene removal in the first 35 minutes of testing is 97%, and, after 83 minutes, the constant rate was 22%. In a concentration of 300 ppm, styrene removal in the first 16 minutes of testing was 97%, and, after 50 minutes, the constant rate was 8%. The results show that the increasing concentration of styrene time of appearance styrene has declined in the output of the system. However, according to studies, the rate of reaction increases with increasing inlet concentration, but the rate of removal efficiency decreases with increasing concentration. This result is related to kinetic effect and blocking the active sites. Increasing the concentration causes the adsorption of more styrene molecules on the photocatalyst surface, and these molecules will block more active sites on the catalyst surface and lead to reduce the hydroxyl radical generation on the photocatalyst surface. In other words, the rate of photodegradation is a function of ZnO amount and hydroxyl radicals, since illumination and amount of catalyst were constant the OH^{o} and O_2^{2-} species attacking the styrene molecules presumably decreased with increasing styrene concentration. Further, as the concentration of styrene increases the photons get intercepted before they can reach the catalyst surface; therefore, the adsorption of photons by ZnO decreases and the catalyst gets deactivated, and consequently the degradation is reduced [43,44].

Studies have shown that with increasing concentrations, the increased probability distribution of pollutants within the pores of the adsorbent and the adsorption rate also increases. Of course, with increasing concentration, the rate of removal of the substrate leak increases because higher concentrations of contaminants may require contact time with the adsorbent [45]. Also, studies on the pollutant oxidation of photocatalyst have shown that the photocatalytic reaction rate depends on the amount of the inlet polluted. Rezaei et al. reported that the rate of the photocatalytic reaction of formaldehyde increases with increasing initial concentration [46].

5. Adsorption Capacity

Catalyst adsorption capacity to the breakthrough was obtained using Eq. (1). In this equation, BC) mass of styrene adsorbed by the catalyst (mg/g), Q) the air flow rate to catalyst (m^3/min), C) the concentration of styrene (mg/m^3), Tbk) breakthrough time.

$$BC = \frac{Q.C.Tbk}{Madsorbent}$$

Table 3. Results of the breakthrough and catalyst adsorption capacity

Sample	Concentration (ppm)	Breakthrough time (min)	Adsorption capacity (mg/g)
Ze	20	26	0.442
	100	15.5	1.318
	300	6	1.53
MZe	20	60	1.020
	100	30	2.552
	300	14	3.572
MZe-ZnO 3%	20	70	1.19
	100	33	2.807
	300	15	3.828
MZe-ZnO 5%	20	75	1.276
	100	36	3.06
	300	18	4.593
MZe-ZnO 10%	20	55	0.935
	100	31	2.637
	300	14	3.57

According to the results presented in Table 3, a styrene breakthrough increases in the catalyst Mze than Ze approximately two times. The adsorption capacity of MZe increases more than two times relative to Ze. This shows that modifying has been made effective by diphenyldichlorosilane. Also, the results of concentration show that with increasing concentration, the adsorption capacity increases in all catalysts. Studies show that with increasing of concentration, more mass of pollutants per unit of time was removed from the air current, so the breakthrough time and saturation of adsorbent ws reduced [47,48]. On the other hand, the ratio of pollutant molecules to the number of active sites on the catalyst surface increased with increasing of concentration, and due to the increased speed of propagation and penetration within the pores, adsorption will occur faster. So full saturation of adsorption sites on the surface of adsorbent occurs in a shorter time [49]. The results also demonstrated that adsorption capacity and breakthrough of MZe-ZnO 3% and MZe-ZnO 5% were higher than MZe. But, a decrease in the adsorption capacity of the MZe-ZnO 10% samples was observed. This can due to lower of specific surface area of MZe-ZnO 10% than MZe. Also, the result indicated that MZe-ZnO 5% had a better adsorption capacity than other in all concentration.

CONCLUSIONS

The results of this study show that zinc oxide nanoparticles immobilized on the MZe can increase the efficiency of photocatalytic decomposition. Increasing the ZnO loading amount resulted in a decrease of styrene adsorption due to decrease in surface area of the photocatalysts, so the photocatalyst with 5 wt% of ZnO content is considered as the optimized photocatalyst.

Based on the results, although this type of zeolite can be a suitable adsorbent to remove styrene from polluted air in such a manner that the concentration amounts to a low flow rate, due to the low surface area compared to other adsorbent such as synthetic zeolites and activated carbon, it's not a good choice for the deployment of pollutant adsorption unless its amount is increased to increase the saturation time or adsorbed and eliminated being altogether. Owing to the abundance of clinoptilolite and the low cost of supply, as well as its unique characteristics, more studies must be conducted on the modification and its application in photocatalytic processes.

ACKNOWLEDGEMENTS

This article was derived from a thesis by Mojtaba Nakhaei Pour as a part of M.sc degree in the field of occupational health engineering. Please add this sentence to Acknowledgements.

FUNDING

This work was supported by the Ahvaz Jundishapur University of Medical Science via grant No. ETRC 9442.

REFERENCES

1. P. Hunter and S. T. Oyama, *Control of volatile organic compound emissions*, John Wiley (2000).
2. US Environmental Protection Agency (USEPA). Sources of indoor air pollution - organic gases (volatile organic compounds, VOCs). USEPA (2013).
3. J. Grzechulska-Damszel, S. Mozia and A. W. Morawski, *Catal. Today*, **156**, 295 (2010).
4. R. Thiruvenkatachari, S. Vigneswaran and I. S. Moon, *Korean J. Chem. Eng.*, **25**, 64 (2008).
5. J. C. Crittenden, J. Liu, D. W. Hand and D. L. Perram, *Water Res.*, **31**, 429 (1997).
6. H. I. De Lasa, B. Serrano and M. Salaices, Photocatal. React. Engin. Springer (2005).
7. J. Saien and A. R. Soleymani, *J. Ind. Eng. Chem.*, **18**, 1683 (2012).
8. T. Charinpanitkul, P. Nartpochananon, T. Satitpitakun, J. Wilcox, T. Seto and Y. Otani, *J. Ind. Eng. Chem.*, **18**, 469 (2012).
9. W. Zhang, Z. Li, Y. Luo and J. Yang, *J. Phys. Chem. C.*, **113**, 8302 (2009).
10. K. Hashimoto, H. Irie and A. Fujishima, *Japan J. Appl. Phys.*, **44**, 8269 (2005).
11. A. Fujishima, X. Zhang and D. A. Tryk, *Surface Science Reports.*, **63**, 515 (2008).
12. M. Muruganandham, Y. Zhang, R. Suri, G.-J. Lee, P.-K. Chen, S.-H. Hsieh, M. Sillanpyää and J. J. Wu, *J. Nanosci. Nanotechnol.*, **15**, 6900 (2015).
13. S. Baruah and J. Dutta, *Sci. Technol. Adv. Mater.* (2009).
14. D. Ehrentraut, H. Sato, Y. Kagamitani, H. Sato, A. Yoshikawa and T. Fukuda, *Progress in Crystal Growth and Characterization of Materials*, **52**, 280 (2006).
15. G. B. Tabrizi and M. Mehrvar, *J. Environ. Sci. Heal, Part A.*, **39**, 3029 (2004).
16. B. Jibril, A. Atta, Y. Al-Waheibi and T. Al-Waheibi, *J. Ind. Eng. Chem.*, **19**, 1800 (2013).
17. M. Safari, M. Nikazar and M. Dadvar, *J. Ind. Eng. Chem.*, **19**, 1697 (2013).

18. T. Komatsu, M. Takasaki, K. Ozawa, S. Furukawa and A. Muramatsu, *J. Phys. Chem. C.*, **117**, 10483 (2013).
19. A. Nezamzadeh-Ejhieh and S. Khorsandi, *J. Ind. Eng. Chem.*, **20**, 937 (2014).
20. N. Mansouri, M. reza Massoudinejad, H. Asilian and A. Mafreshi, *J. Kermanshah. Univ. Med. Sci.*, **14**, 3 (2010).
21. S. Alejandro, H. Valdés, M.-H. Manero and C. A. Zaror, *Water Sci. Technol.*, **66**, 1759 (2012).
22. H. Valdés, S. Alejandro and C. A. Zaror, *J. Hazard. Mater.*, **227**, 34 (2012).
23. M. A. A. Shahmirzadi, S. S. Hosseini and N. R. Tan, *Korean J. Chem. Eng.*, **33**, 3529 (2016).
24. V. R. Posa, V. Annavaram, J. R. Koduru, V. R. Ammireddy and A. R. Somala, *Korean J. Chem. Eng.*, **33**, 456 (2016).
25. C. Ao and S. Lee, *Appl. Catal. B: Environ.*, **44**, 191 (2003).
26. C. Ao and S. Lee, *J. Photochem. Photobio. A: Chem.*, **161**, 131 (2004).
27. H. Ichiura, T. Kitaoka and H. Tanaka, *Chemosphere*, **50**, 79 (2003).
28. P. Zhang, J. Liu and Z. Zhang, *Chem. Lett.*, **33**, 1242 (2004).
29. R.-D. Sun, A. Nakajima, I. Watanabe, T. Watanabe and K. Hashimoto, *J. Photochem. Photobio. A: Chem.*, **136**, 111 (2000).
30. U.S.E.P.A. (USEPA), Sources of indoor air pollution-organic gases (volatile organic compounds, VOCs), http://www.epa.gov/iaq/voc.html.
31. A. Tossavainen, The Scandinavian Journal of Work, Environment & Health, 4 (1978).
32. EPA. Drinking Water Standards Technical Factsheet on: Styrene. Water, 1 (1993).
33. M. Lim, Y. Zhou, B. Wood, Y. Guo, L. Wang, V. Rudolph and G. Lu, *J. Phys. Chem. C.*, **112**, 19655 (2008).
34. TOXICOLOGICAL PROFILE FOR STYRENE, Life Systems, Inc. Under Subcontract to:Clement International Corporation Under Contract No. 205-88-0608. Agency for Toxic Substances and Disease Registry U.S. Public Health Service (1992).
35. Threshold Limit Value For Chemical Substances And Physical Agents And Biological Exposure Indices, American Conferences Of Government Industrial Hygienists (ACGIH) (2012).
36. P. Huttenloch, K. E. Roehl and K. Czurda, *Environ. Sci. Technol.*, **35**, 4260 (2001).
37. H. Asilian, A. Khavanin, M. Afzali and S. Dehestani, *Health Scope.*, **2012**, 7 (2012).
38. Y.-P. Zhu, M. Li, Y.-L. Liu, T.-Z. Ren and Z.-Y. Yuan, *J. Phys. Chem. C.*, **118**, 10963 (2014).
39. M. Hernandez, L. Corona, A. Gonzalez, F. Rojas, V. Lara and F. Silva, *Ind. Eng. Chem Res.*, **44**, 2908 (2005).
40. M. Khatamian and Z. Alaji, *Desalination*, **248**, 286 (2012).
41. J.-C. Chen and C.-T. Tang, *J. Hazard. Mater.*, **142**, 88 (2007).
42. J. Mo, Y. Zhang, Q. Xu, J. J. Lamson and R. Zhao, *Atmosph. Environ.*, **43**, 2229 (2009).
43. R. K. Nath, M. F. M. Zain, A. A. H. Kadhum and A. Kaish, *Construction and Building Materials*, **54**, 348 (2014).
44. D. A. Friesen, L. Morello, J. V. Headley and C. H. Langford, *J. Photochem. Photobio. A: Chem*, **133**, 213 (2000).
45. F. J. DeSilva, Water quality products, 16 (2000).
46. A. Rezaee, H. Rangkooy, A. Jonidi-Jafari and A. Khavanin, *Appl. Surf. Sci*, **286**, 235 (2013).
47. H. C. Wang, H. S. Liang and M. B. Chang, *J. Hazard. Mater.*, **186**, 1781 (2011).
48. T. Mishra, P. Mohapatra and K. M. Parida, *Appl. Catal. B: Environ*, **79**, 3 (2008).
49. E. Rezaei, J. Soltan and N. Chen, *Appl. Catal. B: Environ.*, **136**, 239 (2013).